Dynamic structure factor of the three-dimensional Ising model with purely relaxational dynamics

Pasquale Calabrese,[1,*] Victor Martín-Mayor,[2,†] Andrea Pelissetto,[3,‡] and Ettore Vicari[4,§]
[1]*Scuola Normale Superiore and INFN, Sezione di Pisa, I-56100 Pisa, Italy*
[2]*Departamento de Física Teorica I, Universidad Complutense de Madrid, E-28040 Madrid, Spain*
[3]*Dipartimento di Fisica, Università di Roma La Sapienza and INFN, Sezione di Roma, I-00185 Roma, Italy*
[4]*Dipartimento di Fisica, Università di Pisa and INFN, Sezione di Pisa, I-56100 Pisa, Italy*
(Received 31 January 2003; published 11 July 2003)

We compute the dynamic structure factor for the three-dimensional Ising model with a purely relaxational dynamics (model A). We perform a perturbative calculation in the ϵ expansion, at two loops in the high-temperature phase and at one loop in the temperature magnetic-field plane, and a Monte Carlo simulation in the high-temperature phase. We find that the dynamic structure factor is very well approximated by its mean-field Gaussian form up to moderately large values of frequency ω and momentum k. In the region we can investigate, $k\xi \lesssim 5$, $\omega\tau \lesssim 10$, where ξ is the correlation length and τ is the zero-momentum autocorrelation time, deviations are at most of a few percent.

DOI: 10.1103/PhysRevE.68.016110 PACS number(s): 64.60.Ht, 05.70.Jk, 75.40.Gb, 75.10.Hk

I. INTRODUCTION

The dynamic structure factor $C(k,\omega)$ is a physically interesting quantity that can be directly measured in scattering experiments. Indeed, in neutron-scattering experiments and in Born approximation, $C(k,\omega)$ is proportional to the cross section for inelastic scattering with momentum transfer k and energy transfer ω. At a continuous phase transition the structure factor shows a universal scaling behavior that depends on the dynamic universality class of the system. In this paper we consider the dynamic universality class of the three-dimensional Ising model with purely relaxational dynamics without conservation laws, which is also known as model A. As discussed in Ref. [1], this dynamic universality class should be appropriate to describe the dynamic critical properties of uniaxial magnetic systems in which the energy is not conserved due to the coupling of phonons and of alloys such as β-brass at the order-disorder transition (the energy diffusion rate is very large compared to the relaxation rate of the order parameter and can therefore be neglected, see, Ref. [1]). Note that this universality class does not describe the dynamic behavior of simple fluids and mixtures at the liquid-vapor or mixing transitions because of additional conservation laws [1]. The model-A dynamics for the Ising universality class may also be relevant for the dynamics of quarks and gluons at finite temperature and finite baryon-number chemical potential μ. Indeed, using quantum chromodynamics, which is the current theory of strong interactions, one can argue that in the $T-\mu$ plane there exists an Ising-like continuous transition at the end point of a first-order phase transition line [2,3]. Model A (or model C if one takes into account the baryon-number conservation law [4]) should describe the critical dynamics at this critical point (see also Ref. [5]).

In this paper we compute the structure factor $C(k,\omega)$ for the three-dimensional Ising universality class with purely relaxational dynamics (model A) in equilibrium. Such a model has been extensively studied field theoretically, both in infinite volume [6–10] and in a finite box [11–14]. Here, we consider the ϵ expansion and compute $C(k,\omega)$ to two loops in the high-temperature phase and to one loop in the whole temperature magnetic-field plane. In the high-temperature phase we also perform a Monte Carlo simulation, using the standard Ising model and the Metropolis dynamics [15]. We find that, for moderately large k and ω, $C(k,\omega)$ is very well approximated by its mean-field (Gaussian) expression. In the high-temperature phase, the field-theoretical analysis and the simulation show that corrections to the mean-field behavior are less than 1% for $k\xi \lesssim 5$ and $\omega\tau \lesssim 10$, where ξ is the correlation length and τ is the zero-momentum autocorrelation time. In the low-temperature phase, on the basis of a one-loop field-theoretical analysis, we expect slightly larger corrections, but still of the order of a few percent. Note that our study concerns the scaling behavior of $C(k,\omega)$ in equilibrium, but it should be observed that similar conclusions have been obtained for the nonequilibrium dynamics in which one quenches a disordered system at T_c [16].

The paper is organized as follows. In Sec. II we define the quantities that are computed in the following sections. We report a list of definitions together with some properties that are used in the calculation. In Sec. III we present our field-theoretical results, obtained using the general formalism of Refs. [17–19]. Section IV is devoted to the presentation of the Monte Carlo results. In the Appendix we report some technical details.

II. DEFINITIONS AND BASIC OBSERVABLES

In this paper we consider the equilibrium dynamics for an Ising-like theory with scalar order parameter $\varphi(r,t)$ at temperature T in the presence of a time- and space-independent

*Email address: Pasquale.Calabrese@df.unipi.it
†Email address: Victor@lattice.fis.ucm.es
‡Email address: Andrea.Pelissetto@roma1.infn.it
§Email address: Ettore.Vicari@df.unipi.it

external (magnetic) field H. We consider the connected two-point correlation function of the order parameter

$$G(r,t_1-t_2)\equiv\langle\varphi(r,t_1)\varphi(0,t_2)\rangle_{\rm conn}, \tag{1}$$

where we have assumed to be in equilibrium, so that the correlation function depends only on the difference t_1-t_2. Then, we define its Fourier transform $\tilde{G}(k,t)$ with respect to r,

$$\tilde{G}(k,t)=\int d^d r e^{ik\cdot r}G(r,t), \tag{2}$$

and the structure factor $C(k,\omega)$,

$$C(k,\omega)=\int dt e^{i\omega t}\tilde{G}(k,t). \tag{3}$$

Here, we do not write explicitly the dependence on T and H, which is always understood in the notation. Near the critical point correlations develop both in space and time. They can be characterized in terms of the second-moment correlation length ξ and of the zero-momentum integrated autocorrelation time τ defined by

$$\xi^2\equiv\frac{1}{2d\chi}\int d^d r|r|^2G(r,0)=-\frac{1}{\chi}\left.\frac{\partial\tilde{G}(k,0)}{\partial k^2}\right|_{k^2=0}, \tag{4}$$

$$\tau\equiv\frac{1}{2\chi}\int dt\,\tilde{G}(0,t)=\frac{1}{2\chi}C(0,0), \tag{5}$$

where $\chi\equiv\tilde{G}(0,0)$ is the static magnetic susceptibility. As is well known, for $T\to T_c$ (T_c is the critical temperature) and $H\to 0$, ξ and τ diverge. In the absence of a magnetic field,

$$\xi\sim|T-T_c|^{-\nu},\quad \tau\sim|T-T_c|^{-z\nu}\sim\xi^z, \tag{6}$$

where ν is the usual static exponent and z is a dynamic exponent that depends on the considered dynamics. The static exponents for the three-dimensional Ising universality class are very well determined [20–25], see Ref. [26] for a review. Present-day lattice studies give estimates that can be summarized as follows [26]: $\gamma=1.2372(5)$, $\nu=0.6301(4)$, $\eta=0.0364(5)$, $\alpha=0.110(1)$. The exponent z depends on the dynamics. For model-A dynamics, estimates of z in three dimensions have been obtained by employing several methods. There exist field-theoretical perturbative calculations in different schemes [7,8,10] and Monte Carlo analyses that determine z by studying the equilibrium dynamics at T_c in finite volume [27,28], damage spreading [29,30], the critical relaxation from an ordered state [31,32], hysteresis scaling [33], and the short-time critical dynamics [34]. For experimental determinations see, e.g., Refs. [35,36]. The exponent z turns out to be slightly larger than 2. For instance, $z\approx 2.017$ from the fixed-dimension field-theoretical expansion [10], $z\approx 2.02$ from an analysis interpolating the $4-\epsilon$ and $1+\epsilon$ expansions [7], and $z\approx 2.04$ from the Monte Carlo simulations.

Near the critical point, correlation functions show a scaling behavior. For the static structure factor, neglecting scaling corrections, we have [37,38]

$$\frac{\chi}{\tilde{G}(k,0)}\approx g_{\rm stat}(y;x), \tag{7}$$

where $x\equiv a_0(T-T_c)M^{-1/\beta}$, $y\equiv k^2\xi^2$, $M\equiv\langle\varphi\rangle$ is the time-independent (we only consider the equilibrium dynamics) static magnetization, and a_0 is a normalization factor that is fixed by requiring that $x=-1$ corresponds to the coexistence line. The magnetization M is related to T and H by the equation of state, which, in the critical limit, can be written in the scaling form

$$H=b_0M^\delta f(x), \tag{8}$$

where b_0 is a nonuniversal constant, which is fixed by the condition $f(0)=1$.

The function $g_{\rm stat}(y;x)$ has been extensively studied, both in the high-temperature [39,40] and in the low-temperature phase [41]; see Ref. [26] for an extensive review. In the high-temperature phase, the static function $g^+_{\rm stat}(y)$ is known to $O(\epsilon^3)$ [42], and satisfies $g^+_{\rm stat}(y)=1+y+O(\epsilon^2y^2)$. Its small-momentum expansion in three dimensions has been accurately determined using high-temperature expansion techniques, see, e.g., Refs. [25,26], finding

$$g^+_{\rm stat}(y)=1+y-0.000390(6)y^2+0.0000088(1)y^3+O(y^4). \tag{9}$$

There are also precise estimates of the equation-of-state scaling function $f(x)$ [21,25,43,44].

Equation (7) can be extended to finite values of t. In the critical limit we can write

$$\frac{\chi}{\tilde{G}(k,t)}\approx g(y,s;x) \tag{10}$$

with $s\equiv t/\tau$. We can also define a scaling function for the structure factor:

$$\frac{C(k,\omega)}{2\tau\chi}\approx\mathcal{C}(y,w;x), \tag{11}$$

where $w\equiv\omega\tau$ and

$$\mathcal{C}(y,w;x)=\frac{1}{2}\int ds\,e^{-iws}[g(y,s;x)]^{-1}. \tag{12}$$

We also define an integrated autocorrelation time at momentum k,

$$\tau(k)\equiv\frac{1}{2}\int dt\frac{\tilde{G}(k,t)}{\tilde{G}(k,0)}=\frac{C(k,0)}{2\tilde{G}(k,0)}, \tag{13}$$

and an exponential autocorrelation time

$$\tau_{\rm exp}(k) \equiv - \lim_{|t|\to\infty} \frac{|t|}{\ln \widetilde{G}(k,t)}, \tag{14}$$

which controls the large-t behavior of $\widetilde{G}(k,t)$: $\widetilde{G}(k,t) \sim \exp[-|t|/\tau_{\rm exp}(k)]$ for $|t|\to\infty$. In the scaling limit, neglecting scaling corrections,

$$\frac{\tau(k)}{\tau} \approx \mathcal{T}(y;x) = \mathcal{C}(y,0;x) g_{\rm stat}(y), \tag{15}$$

$$\frac{\tau_{\rm exp}(k)}{\tau(k)} \approx \mathcal{T}_{\rm exp}(y;x) = \frac{1}{|w_0(y;x)| \mathcal{C}(y,0;x) g_{\rm stat}(y)}, \tag{16}$$

where $\pm i w_0(y;x)$ are the zeros of $[\mathcal{C}(y,w;x)]^{-1}$ at fixed y and x on the imaginary w axis that are nearest to the origin $w=0$.

For a Gaussian free theory, we have

$$C(k,\omega)|_{\rm Gaussian} = \frac{2\Omega\chi m^2}{\Omega^2 (m^2+k^2)^2 + \omega^2}, \tag{17}$$

where Ω is an Onsager transport coefficient and $m \equiv 1/\xi$. It follows

$$[\mathcal{C}(y,w;x)]^{-1} = (1+y)^2 + w^2,$$

$$[\mathcal{T}(y;x)]^{-1} = 1+y,$$

$$\mathcal{T}_{\rm exp}(y;x) = 1. \tag{18}$$

For $y\to 0$ and $w\to 0$ the above-defined scaling functions have a regular behavior and one can write

$$[\mathcal{C}(y,w;x)]^{-1} = (1+y)^2 + w^2 + \sum_{m,n=0} c_{n,m}(x) y^n w^{2m},$$

$$[\mathcal{T}(y;x)]^{-1} = 1 + y + \sum_{n=0} t_n(x) y^n,$$

$$\mathcal{T}_{\rm exp}(y;x) = 1 + \sum_{n=0} t_{{\rm exp},n}(x) y^n, \tag{19}$$

with $c_{0,0}(x) = 0$ because of the definition of τ. The expansion coefficients $c_{n,m}(x)$, $t_n(x)$, and $t_{{\rm exp},n}(x)$ parametrize the deviations from the Gaussian behavior (18) in the low-frequency and low-momentum regime.

At the critical point, $T = T_c$, $H = 0$, the structure factor obeys the scaling law

$$C(k,\omega) = \frac{1}{\omega^{(2-\eta+z)/z}} f_C(\omega k^{-z}), \tag{20}$$

with $f_C(\infty)$ finite, which implies that, for $y\to\infty$, $w\to\infty$ keeping $u \equiv w y^{-z/2} = u_0 \omega k^{-z}$ fixed, we have

$$\mathcal{C}(y,w;x) = \frac{f_0}{w^{(2-\eta+z)/z}} f_C(u/u_0), \tag{21}$$

where f_0 is a normalization constant.

For large w at y and x fixed we have

$$\mathcal{C}(y,w;x) \approx c_\infty(y;x) w^{-(2-\eta+z)/z}, \tag{22}$$

where $c_\infty(y;x)$ is finite and x independent for $y\to\infty$. The large-frequency behavior of the structure factor allows us to compute the nonanalytic small-s behavior of $g(y,s;x)$ at y and x fixed. We obtain, for $s\to 0^+$ [45],

$$[g(y,s;x)]^{-1}_{\rm nonanalytic} = g_0(y;x) s^{(2-\eta)/z}, \tag{23}$$

where

$$g_0(y;x) = -\frac{1}{\pi} c_\infty(y;x) \sin(\pi\rho/2) \Gamma(1-\rho), \tag{24}$$

with $\rho \equiv 1 + (2-\eta)/z$. Notice that, since $(2-\eta)/z \approx 0.96$, the nonanalytic small-t behavior of $\widetilde{G}(k,t)$ turns out to be practically indistinguishable from the analytic background.

III. FIELD-THEORETICAL RESULTS

A. Field-theoretical approach

In order to determine the critical behavior of a purely relaxational dynamics without conservation laws, the so-called model-A dynamics, one may start from the stochastic Langevin equation [1,9]

$$\frac{\partial\varphi(r,t)}{\partial t} = -\Omega \frac{\delta \mathcal{H}(\varphi)}{\delta\varphi(r,t)} + \rho(r,t), \tag{25}$$

where $\varphi(r,t)$ is the order parameter, $\mathcal{H}(\varphi)$ is the Landau-Ginzburg-Wilson Hamiltonian

$$\mathcal{H}(\varphi) = \int d^d x \left[\frac{1}{2} (\partial\varphi)^2 + \frac{1}{2} r\varphi^2 + \frac{1}{4!} u \varphi^4 - H\varphi \right], \tag{26}$$

Ω is a transport coefficient [cf. Eq. (17)], and $\rho(t)$ is a Gaussian white noise with correlations

$$\langle \rho(r,t) \rangle = 0, \quad \langle \rho(r_1,t_1) \rho(r_2,t_2) \rangle = \Omega \delta(r_1 - r_2) \delta(t_1 - t_2). \tag{27}$$

The correlation functions generated by the Langevin equation (25) and averaged over the noise ρ can be obtained starting from the field-theoretical action [17–19]

$$S(\varphi,\hat{\varphi}) = \int dt d^d x \left[\hat{\varphi} \frac{\partial\varphi}{\partial t} + \Omega \hat{\varphi} \frac{\delta \mathcal{H}(\varphi)}{\delta\varphi} - \Omega \hat{\varphi}^2 - \ln J(\varphi) \right]. \tag{28}$$

The last term in the action is an appropriate Jacobian term that compensates the contributions of self-loops of response propagators [18,19].

In order to perform the field-theoretical calculation, it is useful to introduce the response function $Y(r,t)$—it gives the linear response to an external magnetic field—defined by

$$Y(r, t_1 - t_2) = \langle \hat{\varphi}(r,t_1) \varphi(0,t_2) \rangle, \tag{29}$$

TABLE I. Numerical values of the coefficients $\overline{r^+_{n,m}}$ for $0 \leqslant m,n \leqslant 3$.

$n \backslash m$	0	1	2	3
0	0	1.03122×10^{-3}	6.19416×10^{-5}	6.51316×10^{-6}
1	-1.04876×10^{-3}	-8.72163×10^{-5}	-1.15844×10^{-5}	-1.92466×10^{-6}
2	4.23375×10^{-5}	7.93211×10^{-6}	1.68104×10^{-6}	3.86236×10^{-7}
3	-2.48539×10^{-6}	-7.51416×10^{-7}	-2.2168×10^{-7}	-6.54471×10^{-8}

(again we have assumed to be in equilibrium so that time-translation invariance holds), its Fourier transform $\tilde{Y}(k,t)$ with respect to r, and its double Fourier transform $R(k,\omega)$ with respect to r and t, defined as $C(k,\omega)$ in Eq. (3). The response function and the two-point correlation function are strictly related. First, the zero-frequency response functions are related to the static correlation functions,

$$\tilde{G}(k,0) = \Omega R(k,0). \tag{30}$$

Moreover, because of the fluctuation-dissipation theorem that holds for the equilibrium dynamics, we have

$$\omega C(k,\omega) = 2\Omega \, \mathrm{Im} \, R(k,\omega). \tag{31}$$

Also the response function $R(k,\omega)$ shows a scaling behavior and one can write

$$\frac{\chi}{\Omega R(k,\omega)} \approx r(y,w;x), \tag{32}$$

neglecting scaling corrections. The function $r(y,w;x)$ is such that

$$r(y,0;x) = 1 + y + O(y^2),$$

$$r(0,w;x) = 1 - iw + O(w^2),$$

$$[r(y,-w;x)]^* = r(y,w;x). \tag{33}$$

Then, it is easy to show by using Eqs. (30) and (31) that

$$r(y,0;x) = g_{\mathrm{stat}}(y;x),$$

$$\mathcal{C}(y,w;x) = -\frac{\mathrm{Im}\, r(y,w;x)}{w|r(y,w;x)|^2}. \tag{34}$$

For a Gaussian theory

$$r(y,w;x) = 1 + y - iw. \tag{35}$$

The behavior of $r(y,w;x)$ for small w and large w is similar to that of $\mathcal{C}(y,w;x)$. For small frequencies and momenta, the scaling function has a regular expansion in powers of w and y:

$$r(y,w;x) = g_{\mathrm{stat}}(y;x) - iw\left[1 + \sum_{n,m} r_{n,m}(x)(iw)^m y^n\right], \tag{36}$$

where the coefficients $r_{n,m}(x)$ are real and parametrize the w dependent deviations from the Gaussian behavior (35). For $w \to \infty$ at fixed y we have

$$r(y,w;x) \approx r^+_\infty(y;x)(-iw)^{(2-\eta)/z}. \tag{37}$$

B. Correlation functions in the disordered phase

In this section we consider the equilibrium dynamics in the high-temperature phase $H=0$, $T>T_c$. In order to determine the two-point correlation function, we have computed the scaling function $r^+(y,w)$ (here and in the following we will not indicate x and add instead a superscript "+" to remind the reader that we refer to the high-temperature phase) and we have then used Eq. (34).

A two-loop calculation in the framework of the ϵ expansion gives

$$r^+(y,w) = g^+_{\mathrm{stat}}(y) - iw[1 + \epsilon^2 A(y,w) + O(\epsilon^3)], \tag{38}$$

where $A(y,w)$ is reported in the Appendix. Note that $A(0,0)=0$ and $A(y,-w)^* = A(y,w)$, as expected from Eq. (33). The static function $g^+_{\mathrm{stat}}(y)$ is known to $O(\epsilon^3)$ [42], and at order ϵ^2 it reads

$$g^+_{\mathrm{stat}}(y) = 1 + y + 10^{-3}\epsilon^2[-3.76012y^2 + 0.095966y^3 - 0.00407101y^4 + O(y^5)] + O(\epsilon^3). \tag{39}$$

Expanding $A(y,w)$ in powers of y and w one obtains the coefficients $r^+_{n,m}$ defined in Eq. (36). We have $r^+_{n,m} = \epsilon^2 \overline{r^+_{n,m}}$, where $\overline{r^+_{n,m}}$ are reported in Table I for $n,m \leqslant 3$. The coefficients $\overline{r^+_{n,m}}$ are rather small, the largest one being of order 10^{-3}, and decrease quite rapidly. The analysis of the coefficients of the expansion of $A(k^2,\omega)$ in powers of k^2 (at fixed ω) shows the presence of a singularity for $w=-3i$. Therefore, we expect asymptotically

$$\overline{r^+_{n,m}} \approx \tfrac{1}{3}\overline{r^+_{n,m-1}}. \tag{40}$$

We have verified numerically this relation, although quantitative agreement is observed only for quite large values of m: for $n=0$, this relation is satisfied at the 10% level only for $m \geqslant 41$. Analogously, the coefficients of the expansion of $A(k^2,\omega)$ in powers of ω become singular for $k^2=-9$, so that asymptotically

$$\overline{r^+_{n,m}} \approx -\tfrac{1}{9}\overline{r^+_{n-1,m}}. \tag{41}$$

Behaviors (40) and (41) can be interpreted in terms of the analytic structure of $R^+(k,\omega)$. If one considers the structure

TABLE II. Numerical values of the coefficients $\bar{c}^{+}_{n,m}$ for $0 \leqslant n,m \leqslant 3$.

$n \backslash m$	0	1	2	3
0	0	0.00212438	-0.000075868	1.22037×10^{-6}
1	0.00104876	0.000951544	9.73059×10^{-7}	-1.87657×10^{-7}
2	-0.0170494	-0.000075777	1.13334×10^{-6}	-1.13131×10^{-8}
3	0.00106254	3.43201×10^{-6}	-2.22548×10^{-7}	1.03457×10^{-8}

factor, it is well known [42,46] that the nearest singularity [47] appearing in $[\tilde{G}(k,0)]^{-1}$ is the three-particle cut at $k = \pm 3im_{\exp}$, where $m_{\exp}$ is the mass gap of the theory. Since in the critical limit $m_{\exp}\xi \approx 1$ [26] with very small corrections (more precisely $m_{\exp}\xi - 1 = -2.00(3)\times10^{-4}$, see Ref. [25]), the nearest singularity to the origin appearing in $g^{+}_{\mathrm{stat}}(y)$ corresponds to $y \approx -9$. In view of relation (41), it is natural to conjecture that the same behavior holds for $R^{+}(k,\omega)$, so that Eq. (41) should approximately hold for the three-dimensional coefficients $r^{+}_{n,m}$ and not only for their two-loop approximation.

Relation (40) is consistent with the idea that the three-particle cut also controls the small-w behavior. In this case it is natural to conjecture that the coefficients of the expansion of $[R^{+}(k,\omega)]^{-1}$ in powers of k^2 have a singularity for $\omega = -3i/\tau_{\exp}(0)$. Thus, turning to the scaling function $r^{+}(y;w)$, we expect a singularity at $w = -3i\tau/\tau_{\exp}(0) \approx -3i$, since, as we shall see, in the critical limit $\tau/\tau_{\exp}(0) \approx 1$. Therefore, we expect relation (40) to be a general property of the three-dimensional coefficients $r^{+}_{n,m}$.

This discussion indicates that $\mathcal{C}(y,0)$ and its w derivatives at $w=0$ have a convergent expansion in y for $|y| \lesssim 9$ and analogously that $\mathcal{C}(0,w)$ and its y derivatives at $y=0$ have a convergent expansion for $|w| \lesssim 3$. Mathematically, this does not tell us much about the convergence of the double expansion that requires to know the singularity structure for both $y,w \neq 0$. At two loops, one can easily verify from the exact expression that $\mathcal{C}(y,w)$ has a convergent double expansion in the whole region $|w|<3$, $|y|<9$, and it is sensible to conjecture that the same is true for the exact expansion. From the results of Table I, one sees quite clearly that the response function $R^{+}(k,\omega)$ is well described by the Gaussian approximation for $|w| \lesssim 3$ and $|y| \lesssim 9$. Deviations should be smaller than 1% in this region. This result is very similar to that obtained for the static structure factor: in that case high-temperature expansions and the Monte Carlo simulations [40] show that the deviations from the Gaussian behavior are less than 0.3% for $y \lesssim 9$.

We now consider the large-frequency behavior. At order ϵ^2 the function $r^{+}_{\infty}(y)$ defined in Eq. (37) turns out to be constant and is given by

$$r^{+}_{\infty}(y) = 1 + 0.00538992\epsilon^2 + O(\epsilon^3). \tag{42}$$

Again the correction term is quite small.

Using fluctuation-dissipation theorem (34), we obtain for the scaling function $\mathcal{C}^{+}(y,w)$:

$$[\mathcal{C}^{+}(y,w)]^{-1} = g_{\mathrm{stat}}(y)^2 + w^2 + \epsilon^2 E(y,w) + O(\epsilon^3), \tag{43}$$

where

$$E(y,w) = 2w(1+y)\,\mathrm{Im}\,A(y,w) + [w^2 - (1+y)^2]\,\mathrm{Re}\,A(y,w). \tag{44}$$

We can then obtain the small-w and small-y behavior. For the coefficients $c^{+}_{n,m}$, see Eq. (19), we obtain $c^{+}_{n,m} = \epsilon^2 \bar{c}^{+}_{n,m}$, where the constants $\bar{c}^{+}_{n,m}$ are reported in Table II for $n,m \leqslant 3$.

Again, we should note that the coefficients $\bar{c}^{+}_{n,m}$ are very small and show the same pattern observed for $\bar{r}^{+}_{n,m}$. We expect that $\mathcal{C}^{+}(y,w)$ has singularities at $y=-9$ and $w = \pm 3i$, so that $|c_{n,m}/c_{n+1,m}| \approx |c_{n,m}/c_{n,m+1}| \approx 9$. Thus, in complete analogy with what observed for the static structure factor and $R^{+}(k,\omega)$, the dynamic $C^{+}(k,\omega)$ is essentially Gaussian in the region $y \lesssim 9$ and $|w| \lesssim 3$.

We also compute the large-frequency behavior. For the coefficients $c^{+}_{\infty}(y)$ and $g^{+}_{0}(y)$, see Eqs. (22) and (23), we obtain

$$c^{+}_{\infty}(y) = 1 - 0.00538992\epsilon^2 + O(\epsilon^3), \tag{45}$$

$$2g^{+}_{0}(y) = 1 + 0.00136716\epsilon^2 + O(\epsilon^3), \tag{46}$$

where, since the corrections are very small, one may simply set $\epsilon = 1$ to obtain a three-dimensional numerical estimate. Therefore, for large w we predict $\mathcal{C}^{+}(y,w) \approx 0.995/w^{1.95}$, which is not very different from the purely Gaussian behavior $\mathcal{C}^{+}_{\mathrm{Gauss}}(y,w) \approx 1/w^2$. Thus, the Gaussian approximation should be a reasonably good approximation even outside the small-w region, $w \lesssim 3$, discussed above. Trusting the above estimate of $c^{+}_{\infty}(y)$ we find that $\mathcal{C}^{+}(y,w)/\mathcal{C}^{+}_{\mathrm{Gauss}}(y,w) = 1.12,\ 1.25,\ 1.41$, respectively, for $w = 10,\ 100,\ 1000$. Thus, quite large values of w are needed in order to observe a significant difference.

Finally we compute the scaling function $\mathcal{T}^{+}_{\exp}(y)$ defined in Eq. (16). For this purpose we need to compute $\tau_{\exp}(k)$ and therefore the large-t behavior of $\tilde{G}(k,t)$. Because of the fluctuation-dissipation theorem, it is equivalent to consider $\tilde{Y}(k,t)$. For $y<3$ we obtain

$$\tilde{Y}(k,t) \approx e^{-s(1+y)}\{1 - \epsilon^2 s A(y, -i(1+y))\}, \tag{47}$$

where $s \equiv t/\tau$, while for $y>3$ we have

$$\tilde{Y}(k,t) \approx e^{-s(1+y)} + \epsilon^2 \frac{27}{8} \frac{e^{-s(y/3+3)}}{s^4 (y-3)^2 (y+9)^3} [1 + O(s^{-1/2})] + O(\epsilon^3). \tag{48}$$

For $y<3$ the correction term exponentiates as expected, and, as a consequence, we obtain

$$\mathcal{C}^+(y,0)[g^+_{\rm stat}(y)]^2 \mathcal{T}^+_{\rm exp}(y) = 1 + \epsilon^2 A(y, -i(1+y)) + O(\epsilon^3). \tag{49}$$

On the other hand, for $y>3$ the correction term decreases with a different exponential factor that dominates for large values of t, suggesting that, at leading order in ϵ, $\tau_{\rm exp}(k)/\tau = (y+9)/3$. In other words, the interaction turns on a new singularity (a three-particle cut) that becomes the leading one for y large enough. However, this is not the end of the story. Indeed, by considering graphs in which one recursively replaces each line with a two-loop watermelon graph, one obtains contributions to $\tilde{Y}(k,t)$ decreasing as $\exp[-s(3^{-n}y + 3^n)]$ (3^n-particle cut), which would be more important for y large enough. These singularities will not probably be the only ones, since we also expect a five-particle cut, a seven-particle cut, etc. On the basis of these results, we expect $\mathcal{T}^+_{\rm exp}(y)$ to have several singularities on the positive real y axis and to become eventually infinite as $y \to \infty$. This is not unexpected since, for $y \to \infty$, $R^+(k,\omega)$ behaves as $\omega^{-(2-\eta)/z}$ and therefore has a branch cut starting at $\omega = 0$.

For $y<3$, we can use Eq. (49) to compute the coefficients $t^+_{{\rm exp},n}$ defined in Eq. (19). We obtain, at order ϵ^2, $t^+_{{\rm exp},0} = 0.00110075\epsilon^2$, $t^+_{{\rm exp},1} = 0.00337789\epsilon^2$, $t^+_{{\rm exp},2} = 0.000217173\epsilon^2$, etc. The coefficients decrease as $t^+_{{\rm exp},n}/t^+_{{\rm exp},n+1} \approx 3$, which reflects the presence of a singularity at $y=3$. Again, for $y<3$ the deviations from a purely Gaussian behavior are very small.

C. Correlation function in the (t,H) plane

In the presence of an external magnetic field H, a one-loop calculation gives

$$r(y,w;x) = g_{\rm stat}(y;x) - iw \left[1 + \epsilon \frac{2}{3+x} B(y,w) + O(\epsilon^2) \right], \tag{50}$$

where $B(y,w)$ is defined in Appendix and

$$g_{\rm stat}(y;x) = 1 + y + \frac{2\epsilon}{3+x} \left[-1 - \frac{y}{12} + \frac{\sqrt{4+y}}{2\sqrt{y}} \ln \frac{\sqrt{4+y} + \sqrt{y}}{\sqrt{4+y} - \sqrt{y}} \right] + O(\epsilon^2). \tag{51}$$

Note that the $O(\epsilon)$ correction vanishes for $x \to \infty$ in agreement with the results of the preceding section. Moreover, the x dependence is very simple and in Eqs. (50) and (51) is always given by the prefactor $2/(3+x)$ that becomes 1 on the coexistence curve $x=-1$. As a consequence, such a prefactor will always appear in this section, multiplying the low-temperature results that will be specified by adding a superscript "$-$" to all definitions. Of course, such a simple x dependence does not hold at higher loops, as it can be seen, for instance, from the two-loop results of Ref. [41] for the static structure factor.

TABLE III. Numerical values of the coefficients $\bar{r}^-_{n,m}$, $\bar{c}^-_{n,m}$, $\bar{t}^-_n$, and $\bar{t}^-_{{\rm exp},n}$ for $n \leqslant 2$ and $m \leqslant 3$.

m	0	1	2	3
$\bar{r}^-_{0,m}$	0	$\frac{1}{48}$	$\frac{1}{192}$	$\frac{1}{640}$
$\bar{r}^-_{1,m}$	$-\frac{5}{192}$	$-\frac{3}{320}$	$-\frac{7}{1920}$	$-\frac{1}{672}$
$\bar{r}^-_{2,m}$	$\frac{11}{1920}$	$\frac{29}{8960}$	$\frac{37}{21504}$	$\frac{115}{129024}$
$\bar{c}^-_{0,m}$	0	$\frac{3}{64}$	$-\frac{17}{1920}$	$\frac{69}{71680}$
$\bar{c}^-_{1,m}$	$\frac{5}{192}$	$\frac{7}{1920}$	$\frac{221}{71680}$	$-\frac{251}{322560}$
$\bar{c}^-_{2,m}$	$\frac{19}{640}$	$-\frac{743}{107520}$	$-\frac{1}{4032}$	$\frac{949}{2838528}$
$\bar{t}^-_m$	0	$\frac{5}{192}$	$\frac{23}{1920}$	$-\frac{697}{215040}$
$\bar{t}^-_{{\rm exp},m}$	$\frac{3}{8} - \frac{1}{2}\ln 2$	$-\frac{65}{64} + \frac{3}{2}\ln 2$	$\frac{1551}{640} - \frac{7}{2}\ln 2$	$-\frac{422211}{71680} + \frac{17}{2}\ln 2$

Again, we note that the corrections to the Gaussian behavior are small, although a factor of 10 larger than the corresponding high-temperature ones. For instance, $\bar{r}^-_{0,1} \approx 0.02$ to be compared with $\bar{r}^+_{0,1} \approx 0.002$. Moreover, the coefficients decrease slower with n and m. This fact can be understood in terms of the singularities of the function $B(y,w)$. A simple analysis shows the presence of singularities for $w=-2i$ and $y=-4$, so that asymptotically

$$\bar{r}^-_{n,m} \approx \tfrac{1}{2} \bar{r}^-_{n,m-1}, \quad \bar{r}^-_{n,m} \approx -\tfrac{1}{4} \bar{r}^-_{n-1,m}. \tag{53}$$

This behavior can be understood on general grounds. Considering the static structure factor, it is known that the nearest singularity in the low-temperature phase is the two-particle cut, $k = \pm 2im_{\rm exp}$, so that $g^-_{\rm stat}(y)$ has a singularity for

$y=-4(m_{\rm exp}\xi)^2\approx -4$, where we have used the fact that in the critical limit $m_{\rm exp}\xi\approx 1$ (more precisely, $m_{\rm exp}\xi\approx 0.96(1)$ [21,48]). As we did for the high-temperature phase, we can thus conjecture that also the singularities of the dynamic functions are controlled by the two-particle cut. Therefore, we expect singularities for $y=-4(m_{\rm exp}\xi)^2\approx -4$ and $w=-2i\tau/\tau_{\rm exp}(0)\approx -2i$, where we have used the fact that $\tau/\tau_{\rm exp}(0)\approx 1$, with corrections of the order of a few percent as discussed below, in the critical limit. Therefore, Eq. (53) should also approximately apply to the three-dimensional coefficients $r^-_{n,m}$.

The above-reported discussion shows that in the region $|y|\lesssim 4$, $|w|\lesssim 2$ the response function can be reasonably approximated by a Gaussian form. Note, however, that, while in the high-temperature phase corrections are expected to be less than 1%, here deviations should be larger.

We have also studied the large-frequency behavior. The coefficient $r_\infty(y;x)$ turns out to be y independent at one loop:

$$r_\infty(y;x)=1-\frac{\epsilon}{3+x}+O(\epsilon^2). \tag{54}$$

Note that the correction is quite large, and thus significant deviations for the Gaussian behavior should be observed as soon as w is large.

Using the fluctuation-dissipation theorem, we can compute at one loop the scaling function $\mathcal{C}(y,w;x)$. For the small-w, small-y coefficients, we obtain

$$c_{n,m}(x)=\frac{2\epsilon}{3+x}\bar{c}^-_{m,n}+O(\epsilon^2),$$

$$t_n(x)=\frac{2\epsilon}{3+x}\bar{t}^-_n+O(\epsilon^2). \tag{55}$$

The coefficients $\bar{c}^-_{m,n}$ and $\bar{t}^-_n$ are reported in Table III for $n\leqslant 2$ and $m\leqslant 3$.

We have also investigated the large-frequency behavior. It is very simple to show, using the above-reported formulas, that at this order $c_\infty(y;x)=1/r_\infty(y;x)$ and $g_0(y;x)=c_\infty(y;x)/2$.

Finally, we consider $\mathcal{T}_{\rm exp}(y;x)$. For this purpose we need to compute the large-t behavior of $\tilde{Y}(k,t)$. We observe a behavior analogous to that observed in the high-temperature phase. For $y<2$,

$$\mathcal{C}(y,0;x)[g_{\rm stat}(y;x)]^2\mathcal{T}_{\rm exp}(y;x)$$
$$=1+\frac{2\epsilon}{3+x}B(y,-i(1+y))+O(\epsilon^2), \tag{56}$$

while for $y>2$ the two-particle cut contribution dominates so that $\tau_{\rm exp}(k)/\tau=2+y/2$. The discussion reported in Sec. III B can also be repeated here. One can easily identify diagrams that decrease as $\exp[-s(2^{-n}y+2^n)]$, indicating that $\mathcal{T}_{\rm exp}(y;x)$ has an infinite number of singularities on the y axis and that it diverges for $y\to\infty$. For small y, we can use Eq. (56) to compute the small-y expansion coefficients $t_{{\rm exp},n}(x)$. We have

TABLE IV. Results of the Monte Carlo simulations.

	(a)	(b)	(c)	(d)
L	64	64	128	128
β	0.215	0.219	0.2204	0.2210
$N_{\rm it}$	30×10^6	8×10^6	9×10^6	4×10^6
ξ	4.4598(9)	8.081(6)	13.050(7)	19.739(14)
τ	19.38(11)	64.9(9)	176(4)	420(23)

$$t_{{\rm exp},n}(x)=\frac{2\epsilon}{3+x}\bar{t}^-_{{\rm exp},n}+O(\epsilon^2). \tag{57}$$

Numerical values are reported in Table III. Note that $\tau_{\rm exp}(0)/\tau=1+\bar{t}^-_{{\rm exp},0}\approx 1+0.0284\epsilon$, and thus we expect this ratio to be 1 with corrections of the order of a few percent.

IV. MONTE CARLO RESULTS

We determine the dynamic structure factor $C(k,\omega)$ and the scaling function $\tilde{G}(k,t)$ in the high-temperature phase $H=0$, $T>T_c$ for small values of k—as we shall see, we are able to reach $k\approx 10/\xi$—by means of a large-scale Monte Carlo simulation. We consider the Ising model on a cubic lattice, i.e., the Hamiltonian

$$\mathcal{H}=-\beta\sum_{\langle ij\rangle}\sigma_i\sigma_j, \tag{58}$$

where $\beta\equiv 1/T$, $\sigma_i=\pm 1$, and the summation is over all nearest-neighbor pairs $\langle ij\rangle$. We measure the correlation function

$$\tilde{G}(k,t)=\frac{1}{3}\sum_{x,y,z}(e^{iqx}+e^{iqy}+e^{iqz})\langle\sigma_{0,0,0}(t=0)\sigma_{x,y,z}(t)\rangle, \tag{59}$$

for four different values of L and β: (a) $L=64$, $\beta=0.215$; (b) $L=64$, $\beta=0.219$; (c) $L=128$, $\beta=0.2204$; (d) $L=128$, $\beta=0.221$. Of course, in Eq. (59) $q=2\pi n/L$ where n is an integer. For each β and L we first reached equilibrium by running 20 000 Swendsen-Wang iterations, then we collected $N_{\rm it}$ iterations using the Metropolis algorithm [49]. The results of the simulations are reported in Table IV. There we report the number of iterations $N_{\rm it}$, the second-moment correlation length ξ (for the $L=128$ lattices we report more precise results of Ref. [40]), and the autocorrelation time τ. Note that all lattices have $L/\xi\gtrsim 6$, a condition that usually ensures that finite-size effects are reasonably small (for static quantities corrections are less than 1%).

The correlation length ξ has been determined by using a discretized form of Eq. (4):

$$\xi^2=\frac{\chi/F-1}{4\sin^2(\pi/L)}, \tag{60}$$

where $F=\tilde{G}(k,0)$ with $k=(2\pi/L,0,0)$. The integrated autocorrelation time τ and also the autocorrelation times $\tau(k)$

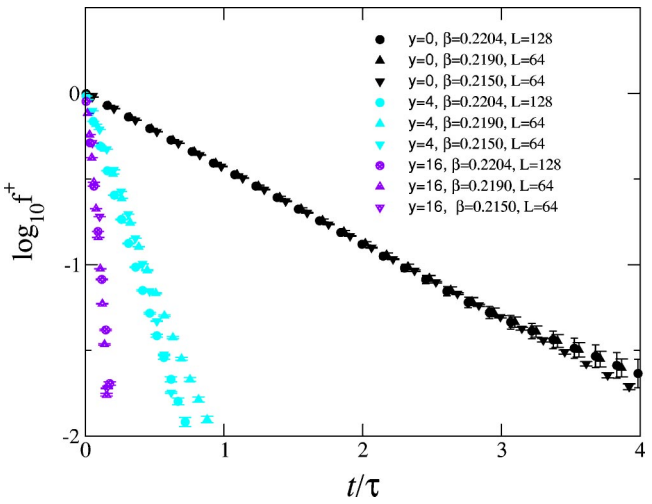

FIG. 1. The scaling function $f^+(y,s)$. We report results for lattices (a), (b), and (c) and for three different values of y.

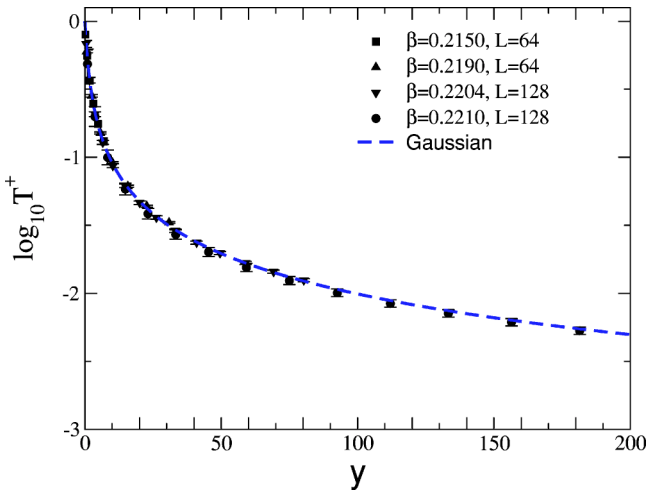

FIG. 2. Scaling plot of $\mathcal{T}(y)$ vs $y \equiv k^2\xi^2$.

considered below have been determined using the self-consistent method of Ref. [50]:

$$\tau(k) = \frac{1}{2} + \sum_{t=1}^{M(k)} \frac{\tilde{G}(k,t)}{\tilde{G}(k,0)}, \tag{61}$$

where t is the Monte Carlo time in sweeps and the cutoff $M(k)$ is chosen self-consistently so that $6\tau(k) < M(k) \leq 6\tau(k)+1$. Since $\tilde{G}(k,t)$ decays exponentially, this choice makes the systematic error due to the truncation small, keeping the statistical variance small at the same time; see Ref. [50] for a discussion.

First, we check that $\tau \approx \xi^z \approx |T-T_c|^{-z\nu}$. Using the precise estimate $\beta_c = 0.22165459(10)$ of Ref. [22], we obtain from a least-square fit $z = 2.10(2)$ including all data and $z = 2.11(5)$ discarding the estimate of τ for lattice (a). This result is in reasonable agreement with the estimates reported in Sec. II, if we take into account that we quote here only the statistical error. The systematic error due to corrections to scaling and to neglected finite-size effects is probably larger.

Then, we determine the correlation function $\tilde{G}(k,t)$. In Fig. 1 we report the function

$$f^+(y,s) \equiv \frac{g^+(y,0)}{g^+(y,s)} \approx \frac{\tilde{G}(k,t)}{\tilde{G}(k,0)}, \tag{62}$$

for three different values of $y \equiv k^2\xi^2$, $y = 0,4,16$, as computed from lattices (a), (b), and (c). We have not included the results for lattice (d), because they have much larger errors. In order to obtain $\tilde{G}(k,t)$ for a given $k \neq 2\pi n/L$, we have performed a linear interpolation, using two nearby values of k. First, we observe reasonable scaling: corrections due to the finite values of ξ and L are under control, although they increase as y increases. For $y=0$ the results for the three different lattices agree within a few percent, while for larger values of y we observe larger discrepancies. In particular, for $y=4$ and $y=16$, the estimates of $f^+(y,s)$ obtained from lattice (b) are always larger than those obtained from (a) and (c), the discrepancy being of the order of 20% when $f^+(y,s) \approx 10^{-1}$ and 80% when $f^+(y,s) \approx 10^{-2}$. These differences are probably finite-size effects, since (a) and (c) have $L/\xi \gtrsim 10$, while $L/\xi \approx 8$ for (b).

It is also remarkable that the plot of $\ln f^+(y,s)$ is a straight line, indicating that $f^+(y,s)$ is quite precisely a pure exponential. No deviations can be observed in Fig. 1. Therefore,

$$\tilde{G}(k,t) \approx \tilde{G}(k,0) \exp[-t/\tau_{\rm exp}(k)], \tag{63}$$

within the precision of our results. This behavior appears to be well satisfied in the region that we can safely investigate, i.e., $1/10 \lesssim t/\tau(k) \lesssim 4$ and $k\xi \lesssim 5$. Therefore, the dynamic structure factor is well approximated by a Lorentzian in the region of not too large frequencies, i.e., for $\omega\tau(k) \lesssim 10$.

Then, we consider the scaling function $\mathcal{T}(y)$ that encodes the k dependence of $\tau(k)$. In Fig. 2 we report our numerical results. Again, we observe good scaling up to quite large values of y. In the figure, we also report the Gaussian prediction $\mathcal{T}(y) = 1/(1+y)$. It can be seen that the Gaussian approximation describes very well the numerical data. This result should have been expected on the basis of the results of Sec. III where we showed that the deviations from a Gaussian behavior are very small in the small-y regime $y \lesssim 9$, and should remain small even for larger y. For instance, using the data with largest y reported in Fig. 2, we estimate $\mathcal{T}(y) = 0.0053(3)$ for $y = 181$, to be compared with the Gaussian prediction 0.0055. Thus, in the range $y \lesssim 200$, the discrepancy should be at most 4–10 %.

Finally, we consider the function $\mathcal{T}^+_{\rm exp}(y)$. In order to compute $\tau_{\rm exp}(k)$ we define an effective quantity

$$\tau_{\rm eff}(t;k) \equiv -\left[\ln \frac{\tilde{G}(k,t+1)}{\tilde{G}(k,t)}\right]^{-1}. \tag{64}$$

The exponential autocorrelation time $\tau_{\rm exp}(k)$ is obtained from $\tau_{\rm eff}(t;k)$ by letting t go to infinity. In practice, we can only compute $\tau_{\rm eff}(t;k)$ up to t of the order of $(1-2)\times\tau(k)$, since errors increase rapidly. In Fig. 3 we report the ratio $\tau_{\rm eff}(t;k)/\tau(k)$ for $t = \tau(k)$ for lattice (c), which is the only

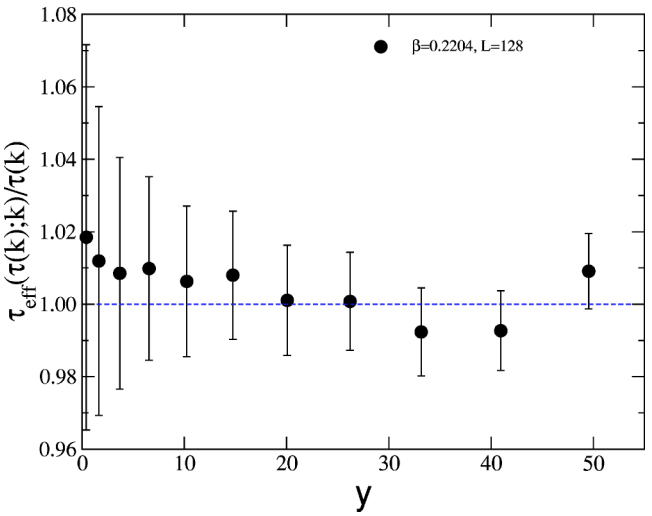

FIG. 3. Ratio $\tau_{\rm eff}(t;k)/\tau(k)$ vs $y\equiv k^2\xi^2$, for $t=\tau(k)$. Results for lattice (c), $L=128$, $\beta=0.2204$.

one that allows us to reach large values of y. We observe $\tau_{\rm eff}(t;k)\approx\tau(k)$ within the precision of our results. It is tempting to conclude that $\tau_{\rm exp}(k)\approx\tau(k)$ for $y<50$, but this is in contrast with the theoretical results of Sec. III B. Indeed, we showed there that $\tau_{\rm exp}(k)\approx\tau(k)$ with very small corrections for $y<3$, but we noticed that this relation breaks down for larger values of y. For instance, for $y>3$, our two-loop calculation gives $\tau_{\rm exp}(k)/\tau(k)=(3+3y)/(9+y)$, which is significantly larger than 1 for $y>3$. As we already discussed this prediction should not be taken seriously, unless y is close to 3, since other singularities should be present, and indeed we expect $\tau_{\rm exp}(k)/\tau(k)$ to diverge as $k\to\infty$. Therefore, our numerical data show that the asymptotic large-t behavior sets in only for large values of t, i.e., for $t\gg\tau(k)$, where the correlation function $\tilde{G}(k,t)$ is very small. Therefore, even if Eq. (63) breaks down for $y\gtrsim 3$ and t large, it still represents a very good approximation (even for $y\approx 50$) for the values of t for which $\tilde{G}(k,t)$ is sizeable.

ACKNOWLEDGMENTS

This work was partly supported by MCyT (Spain), Project Nos. FPA2001-1813 and FPA2000-0956.

APPENDIX: INTEGRALS ENTERING THE FIELD-THEORETICAL CALCULATIONS

In this appendix we report some integrals that enter the perturbative field-theoretical calculations.

In the two-loop calculation of the response scaling function in the high-temperature phase, cf. Eq. (38), one needs to compute the function

$$A(k^2,\omega)=\tfrac{2}{27}N_d^{-2}[I(k,\omega)-I(0,0)], \tag{A1}$$

with (dimensional regularization near four dimensions is understood)

$$I(k,\omega)=\int_0^\infty dt e^{i\omega t}\int\frac{d^dp_1}{(2\pi)^d}\frac{d^dp_2}{(2\pi)^d}\prod_{i=1}^3\frac{1}{p_i^2+1}e^{-t\sum_i(p_i^2+1)}, \tag{A2}$$

where $p_3=k-p_1-p_2$, and $N_d=2/[(4\pi)^{d/2}\Gamma(d/2)]$. The integral $I(k,\omega)$ can be written in the form

$$N_d^{-2}I(k,\omega)=\frac{1}{3}\frac{1}{(4\pi)^dN_d^2}\int_0^1t^2dt\int_0^\infty dse^{-s}s^{3-d}e^{i\omega s(1-t)/3}\times\int_0^1u\,du\,dv\frac{e^{-s(Q/\Delta)k^2}}{\Delta^{d/2}}, \tag{A3}$$

where

$$\Delta=t^2u[1-u+uv(1-v)]+\tfrac{1}{3}(1-t^2), \tag{A4}$$

$$Q=t^3u^2(1-u)v(1-v)+\frac{1-t}{3}t^2u[1-u+uv(1-v)]+\frac{(1-t)^2}{9}t+\frac{(1-t)^3}{27}. \tag{A5}$$

We will also need the singularity structure of $A(k^2,\omega)$. For this purpose, we will determine the large-t behavior of $\tilde{A}(k^2,t)$, which is the Fourier transform with respect to ω of $A(k^2,\omega)$. This behavior can easily be derived from Eq. (A2). Setting $p_1=k/3+q_1/\sqrt{t}$, $p_2=k/3+q_2/\sqrt{t}$, $p_3=k/3+q_3/\sqrt{t}$, we obtain that for $t\to\infty$,

$$\begin{aligned}\tilde{A}(k^2,t)&\approx\frac{2}{27}N_d^{-2}t^{-d}e^{-k^2t/3-3t}\frac{1}{(k^2/9+1)^3}\times\int\frac{d^dq_1}{(2\pi)^d}\frac{d^dq_2}{(2\pi)^d}e^{-(q_1^2+q_2^2+q_3^2)}[1+O(t^{-1/2})]\\&=\frac{1}{(k^2/9+1)^3}\frac{(1/3)^{d/2}}{54}\Gamma^2(d/2)t^{-d}e^{-k^2t/3-3t}[1+O(t^{-1/2})]\\&\approx\frac{1}{(k^2+9)^3}\frac{3e^{-k^2t/3-3t}}{2t^4}[1+O(t^{-1/2})]+O(\epsilon).\end{aligned} \tag{A6}$$

This result implies the presence of a branching cut in $A(k^2,\omega)$, starting at $\omega=-i(3+k^2/3)$.

The one-loop expression of the response function in the ordered phase, cf. Eq. (50), is written in terms of the function

$$B(k^2,\omega)=N_d^{-1}[J(k,\omega)-J(0,0)], \tag{A7}$$

where

$$J(k,\omega)=\int_0^\infty dt e^{i\omega t}\int \frac{d^d p_1}{(2\pi)^d}\prod_{i=1}^{2}\frac{1}{p_i^2+1}e^{-t\sum_i^2 (p_i^2+1)}, \tag{A8}$$

with $p_2=k-p_1$. The function $B(k^2,\omega)$ can be written in the form

$$B(k^2,\omega)=\frac{1}{2}\int_0^1 t\,dt\,du \times\frac{i2\omega(1-t)-[1-t^2+4t^2u(1-u)]k^2}{4+[1-t^2+4t^2u(1-u)]k^2-2i\omega(1-t)}. \tag{A9}$$

Such an integral can be computed exactly obtaining

$$B(k^2,\omega)=-\frac{1}{2}+\frac{1}{k^2}\ln\frac{4+2i\omega+k^2}{4-2i\omega+k^2}+\frac{2i}{\omega}\sqrt{\frac{4+k^2}{k^2}} \times\ln\frac{\sqrt{4+k^2}-\sqrt{k^2}}{\sqrt{4+k^2}+\sqrt{k^2}}-\frac{1}{k^2}\ln\frac{4\omega^2+(4+k^2)^2}{16} +\frac{2}{\omega k^2}F\left(\ln\frac{F-\omega}{F+\omega}+\ln\frac{F+\omega+ik^2}{F-\omega-ik^2}\right), \tag{A10}$$

with $F\equiv\sqrt{\omega^2+2i\omega k^2-k^2(4+k^2)}$. It is easy to see using this exact expression or repeating the argument presented for $A(k^2,\omega)$ that $B(k^2,\omega)$ is singular for $\omega=-i(2+k^2/2)$.

[1] P.C. Hohenberg and B.I. Halperin, Rev. Mod. Phys. **49**, 435 (1977).
[2] M.A. Halasz, A.D. Jackson, R.E. Shrock, M.A. Stephanov, and J.J. Verbaarschot, Phys. Rev. D **58**, 096007 (1998).
[3] J. Berges and K. Rajagopal, Nucl. Phys. B **538**, 215 (1999).
[4] B. Berdnikov and K. Rajagopal, Phys. Rev. D **61**, 105017 (2000).
[5] Sz. Borsányi, A. Patkós, D. Sexty, and Zs. Szép, Phys. Rev. D **64**, 125011 (2001).
[6] R. Bausch and H.K. Janssen, Z. Phys. B **25**, 275 (1976).
[7] R. Bausch, V. Dohm, H.K. Janssen, and R.P.K. Zia, Phys. Rev. Lett. **47**, 1837 (1981).
[8] N.V. Antonov and A.N. Vasil'ev, Teor. Mat. Fiz. **60**, 59 (1984) [Theor. Math. Phys. **60**, 671 (1984)].
[9] H.K. Janssen, in *From Phase Transition to Chaos*, edited by G. Györgyi, I. Kondor, L. Sasvári, and T. Tel (World Scientific, Singapore, 1992), p. 68.
[10] V.V. Prudnikov, A.V. Ivanov, and A.A. Fedorenko, Pis'ma Zh. Éksp. Teor. Fiz. **66**, 793 (1997) [JETP Lett. **66**, 835 (1997)].
[11] H.W. Diehl, Z. Phys. B: Condens. Matter **66**, 211 (1987).
[12] J.C. Niel and J. Zinn-Justin, Nucl. Phys. B **280**, 355 (1987).
[13] Y.Y. Goldschmidt, Nucl. Phys. B **285**, 519 (1987).
[14] U. Ritschel and H.W. Diehl, Nucl. Phys. B **464**, 512 (1996).
[15] Equivalently, we could have used the heat-bath (or Glauber) dynamics that is also expected to belong to the dynamic universality class of model *A*.
[16] P. Calabrese and A. Gambassi, Phys. Rev. E **65**, 066120 (2002); **66**, 066101 (2002).
[17] P.C. Martin, E.D. Siggia, and H.A. Rose, Phys. Rev. A **8**, 423 (1973).
[18] R. Bausch, H.K. Janssen, and H. Wagner, Z. Phys. B **24**, 113 (1976).
[19] C. De Dominicis and L. Peliti, Phys. Rev. B **18**, 353 (1978).
[20] R. Guida and J. Zinn-Justin, J. Phys. A **31**, 8103 (1998).
[21] M. Campostrini, A. Pelissetto, P. Rossi, and E. Vicari, Phys. Rev. E **60**, 3526 (1999).
[22] H.W.J. Blöte, L.N. Shchur, and A.L. Talapov, Int. J. Mod. Phys. C **10**, 1137 (1999).
[23] M. Hasenbusch, Int. J. Mod. Phys. C **12**, 911 (2001).
[24] P. Butera and M. Comi, Phys. Rev. B **65**, 144431 (2002).
[25] M. Campostrini, A. Pelissetto, P. Rossi, and E. Vicari, Phys. Rev. E **65**, 066127 (2002).
[26] A. Pelissetto and E. Vicari, Phys. Rep. **368**, 549 (2002).
[27] S. Wansleben and D.P. Landau, Phys. Rev. B **43**, 6006 (1991).
[28] H. Heuer, J. Phys. A **25**, L567 (1992).
[29] U. Gropengiesser, Physica A **213**, 308 (1995).
[30] P. Grassberger, Physica A **214**, 547 (1995); **217**, 227(E) (1995).
[31] D. Stauffer and R. Knecht, Int. J. Mod. Phys. C **7**, 893 (1996).
[32] D. Stauffer, Physica A **244**, 344 (1997).
[33] G.P. Zheng and J.X. Zhang, Phys. Rev. E **58**, R1187 (1998).
[34] A. Jaster, J. Mainville, L. Schülke, and B. Zheng, J. Phys. A **32**, 1395 (1999).
[35] D.P. Belanger, B. Farago, V. Jaccarino, A.R. King, C. Lartigue, and F. Mezei, J. Phys. (Paris), Colloq. **49**, 1229 (1988).
[36] M.T. Hutchings, M.P. Schulhof, and H.J. Guggenheim, Phys. Rev. B **5**, 154 (1972).
[37] M.E. Fisher and R.J. Burford, Phys. Rev. **156**, 583 (1967).
[38] H.B. Tarko and M.E. Fisher, Phys. Rev. Lett. **31**, 926 (1973); Phys. Rev. B **11**, 1217 (1975).
[39] M. Campostrini, A. Pelissetto, P. Rossi, and E. Vicari, Phys. Rev. E **57**, 184 (1998).
[40] V. Martín-Mayor, A. Pelissetto, and E. Vicari, Phys. Rev. E **66**, 026112 (2002).
[41] M. Combescot, M. Droz, and J.M. Kosterlitz, Phys. Rev. B **11**, 4661 (1975).
[42] A.J. Bray, Phys. Rev. B **14**, 1248 (1976).
[43] R. Guida and J. Zinn-Justin, Nucl. Phys. B **489**, 626 (1997).
[44] J. Engels, L. Fromme, and M. Seniuch, Nucl. Phys. B **655**, 277 (2003).
[45] Here we use the fact that the integral $\int d\omega/(2\pi)|\omega|^x\exp(i\omega t)$ is given by $-\pi^{-1}\sin(\pi x/2)\Gamma(1+x)|t|^{-1-x}$ for $x>-1$.
[46] R.A. Ferrell and D.J. Scalapino, Phys. Rev. Lett. **34**, 200 (1975).
[47] Note that, beside the three-particle cut, $\tilde{G}(k,0)$ shows an additional singularity, the one-particle pole at $k=\pm im_{\rm exp}$. However, such a point is a simple zero—therefore *not* a singularity—of the inverse $[\tilde{G}(k,0)]^{-1}$.
[48] M.E. Fisher and S.-Y. Zinn, J. Phys. A **31**, L629 (1998).

[49] We used the Metropolis algorithm with *sequential* updating of the sites. At variance with the Metropolis algorithm with random updating, this dynamics is not reversible (it does not satisfy detailed balance). Nonetheless, it is commonly accepted that in the critical limit these two dynamics should both belong to the dynamic universality class of model *A* that describes a *reversible* diffusive dynamics without conservation laws.

[50] N. Madras and A.D. Sokal, J. Stat. Phys. **50**, 109 (1988).